MECHANICAL PROPERTIES OF RUBBER COMPOSITE MATERIALS FILLED WITH NANOFILLERS

Martin Vašina[1], Marek Pöschl[2], Lumír Hružík[1], Adam Bureček[1], Kamila Kotrasová[3], Eva Kormaníková[3]

[1]VŠB – Technical University of Ostrava, Department of Hydromechanics and Hydraulic Equipment Faculty of Mechanical Engineering, 17 Listopadu 2172/15, 708 00 Ostrava, Czech Republic
[2]Tomas Bata University in Zlín, Department of Production Engineering, Faculty of Technology, Vavrečkova 275, 760 01 Zlín, Czech Republic
[3]Technical University of Košice, Department of Structural Mechanics, Institute of Structural Engineering, Vysokoškolská 4, 042 00 Košice, Slovakia

Corresponding author: Martin Vašina, martin.vasina@vsb.cz

Abstract: The aim of this paper is to investigate mechanical properties of different types of rubber composite materials that are filled with Cloisite and carbon black nanofillers. Mechanical properties of the rubber composites were investigated by means of tensile testing, viscoelastic behaviour, Shore hardness, rebound resilience and vibration damping measurements. It was found in this study that the rubber composition has a significant influence on the above-mentioned properties. It can be concluded that the rubber stiffness is generally increasing with increasing the content of the applied nanofillers. The mechanical vibration damping analysis also verified higher stiffness of the rubber composites. A better ability to damp mechanical vibration was reflected in a shift of the first resonance peak position to lower excitation frequencies.
Key words: Rubber composite, nanofiller, vibration damping, tensile testing, viscoelasticity, hardness.

1. INTRODUCTION

Rubber products are applied in many areas at the present time, e.g. for production of tires, hoses, seals, conveyor belts, rubber boots and damping elements (Chandrasekaran, 2010). Rubber properties are significantly influenced by their composition. Rubber materials consist of natural or synthetic rubbers. The natural rubber is a high molecular mass polymeric substance which exhibits high tensile strength as a gum vulcanizate (Ghari and Jalali-Arani, 2016). It is frequently used in rubber industry, but its low heat resistance and wide distribution curve (i.e. chains of different lengths in a system) characterize this rubber. Synthetic rubbers are produced by emulsion polymerization in a reactor. There are different types of these rubbers, e.g. synthetic rubbers for general utilizations (e.g. SBR, BR and IR rubbers) and special purposes (e.g. EPM, EPDM, CR and NBR rubbers). In general, the natural or synthetic rubbers aren´t separately used in order to improve their properties. For this reason, different ingredients (fillers, vulcanization agents, UV stabilizers etc.) are added to these rubbers. These rubber mixtures are plastic and formable. During heating to high temperatures (t>100°C), the rubber mixture is changed into elastic rubber, i.e. vulcanizate (Gent, 2012; Limper, 2012). This vulcanizate is resistant to deformation, wear and chemical substances. A rubber mixture composition is expressed in phr units (i.e. parts by weight, per 100 parts of rubber) (Valaderes et al., 2006).

Fillers belong to significant ingredients of rubber mixtures, because they modify physical and mechanical properties of rubber mixtures and reduce their price. The fillers are divided according to primary particle sizes. Active fillers (particle diameter d=(0.01÷0.10) μm) absorb more mechanical energy and improve tensile strength, structural strength and abrasive resistance. Semi active fillers of the particle diameter d=(0.1÷1.0) μm improve tensile strength and structural strength, but their abrasive resistance is worse compared to the active fillers. They don´t improve properties of rubber mixtures and are only applied in order to reduce production costs of the mixtures (Eckhoff, 2016; Chandrasekeran, 2010). The filler particles of the diameter d>10 μm can lead to crack formation. Therefore, such large particles are not used in rubber mixtures. Furthermore, the fillers are divided according to the colour (i.e. light and dark), the shape of primary particles (e.g. tabular, flaky and cubic) and their origin (i.e. natural or synthetic). There are applied different types of nanofillers at the present time, e.g. carbon black, silica, clay, organically modified clay, nano-graphite and nanotubes (Thomas et al., 2014).

The aim of this paper is to investigate the effect of rubber composition on mechanical properties. Investigated rubber composite materials were filled

with Cloisite and carbon black nanofillers of different concentrations. Based on a suitable volume ratio of these nanofillers, it is possible to obtain a significant synergy effect on physical and mechanical properties of the rubber composite materials.

2. INVESTIGATED MATERIALS

2.1 Material Composition

The designation and composition of the investigated rubber mixtures are shown in Table 1. Styrene-butadiene rubber of SBR–1500 type (Synthos Kralupy a.s., Kralupy nad Vltavou, Czech Republic) containing 23.5% styrene was used as the basic component of the manufactured rubber mixtures that were filled with Cloisite 20A (BYK Additives & Instruments GmbH, Wesel, Germany) and carbon black N 320 (CS CABOT spol. s r.o., Valašské Meziříčí, Czech Republic) nanofillers. The Cloisite 20A nanoclay is a layered silicate that is applied in rubber mixtures in order to improve mechanical and barrier properties and to reduce rubber flammability (Wu et al., 2001). The applied carbon black N 320 nanofiller consisted of the particles of the diameter d=(0.026÷0.030)μm (Lee et al., 2014; Cox, 2012) and is used to absorb ultraviolet radiation.

Table 1. Designation and composition (in phr units) of the tested rubber mixtures

Ingredient type	Rubber mixture designation				
	0_0	50_0	40_10	30_20	20_30
SBR-1500	100	100	100	100	100
N 320	0	50	40	30	20
Cloisite 20A	0	0	10	20	30
ZnO	3	3	3	3	3
Stearin	1	1	1	1	1
TBBS	1	1	1	1	1
Sulphur	1.75	1.75	1.75	1.75	1.75

2.2 Rubber Processing

The rubber mixtures were prepared by two-stage mixing whose time record is shown in Table 2.

Table 2. Time record of rubber mixing process

Mixing equipment	Sequence of additive feeding	Adding time (min)
Pommini Farrel kneader	SBR-1500	0:00
	ZnO + Stearin	1:00
	1st half of N 320	2:00
	2nd half of N 320 + 1st half of Cloisite 20A	3:00
	2nd half of Cloisite 20A	4:00
	Mixture drainage	8:30
Farrel double roller	Mixture from 1st stage	0:00
	TBBS + Sulphur	3:00
	Rubber contraction	7:00

The rubber mixtures were also filled by vulcanization activators (i.e. Stearin and zinc oxide ZnO), vulcanization accelerator TBBS (i.e. N-t-butyl-2-benzothiazole sulfenamide) and Sulphur, as shown in Table 1.

The first stage was performed on a Pommini Farrel kneader at the temperature of 85°C and the speed of 99rev/min. After this immixture, the mixture was drained out from the kneader. Subsequently, vulcanization accelerator TBBS and Sulphur were added to the mixture on a Farrel double roller. The second stage was realized at the temperature of 70°C and the speed ratio of 12/15 of both rollers. After this process, the rubber mixture was stored for its further processing for a period of 24 hours at an ambient temperature of 22°C. The specimens for testing of required properties were subsequently pressed from the rubber mixture at the temperature of 165°C.

3. METHODS

3.1 Tensile Testing

Tensile properties of the tested rubber samples were investigated on a T10D tensile testing machine from Alpha Technology according ISO 37 standard at the ambient temperature of 22°C. Eight specimens of the given rubber type (see Table 1) were strained at the test speed of 50mm/min in this case. Average values of measured quantities and their standard deviations were subsequently evaluated.

3.2 Hardness

The Shore A hardness was measured on rubber samples of the thickness t=6 mm according ISO 7619 standard at the ambient temperature of 22°C. Consequently, the hardness median was obtained from five measured values.

3.3 Rebound Resilience

The rebound resilience was measured according ISO 4662 standard. Samples of the thickness t=6 mm were examined in this case. The average value of the rebound resilience and its standard deviation were subsequently determined from three measured values. These measurements were carried at the ambient temperature of 22°C.

3.4 Dynamical Mechanical Analysis

Dynamical mechanical analysis was realized on Mettler Toledo DMA 1 equipment in tensile mode for the investigated rubber samples whose geometrical dimensions were 10×5×1 mm (length×width×thickness). Viscoelastic parameters (i.e. storage modulus E´, loss modulus E´´ and loss factor tanδ) were determined in two different ways. Firstly, the frequency sweep was measured at the constant deformation of 10 μm with

the varying frequency from 0Hz to 150Hz. Secondly, the deformation sweep was investigated with the varying sample deformation from 0µm to 200µm. The storage modulus E´ defines the energy stored in the specimen when a force field is applied (Reyes-Melo et al., 2004). The loss modulus E´´ is related to energy dissipation. The loss factor tanδ is given by the ratio of the loss modulus to the storage modulus (tanδ=E´´/E´) and characterizes the degree of energy dissipation or material damping.

3.5 Mechanical Vibration Testing

Vibration damping properties of the tested rubber samples were investigated by the forced oscillation method using a BK 4810 (Brüel & Kjær, Nærum, Denmark) mini-shaker in combination with a BK 3560-B-030 signal pulse multi-analyzer and a BK 2706 power amplifier at the frequency range of 2÷3200 Hz (see Figure 1). Sine waves were generated by the mini-shaker.

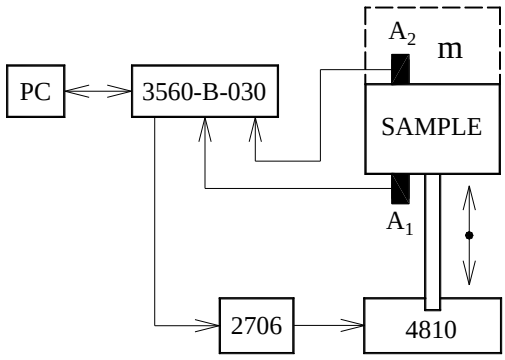

Fig. 1. Schematic diagram of measuring device

The material ability to damp harmonically excited mechanical vibration can be expressed by the displacement transmissibility T_d (Rao, 2005; Mallik et al., 1999), which is defined by the equation (1):

$$T_d=y_2/y_1=[(1+(2\zeta r)^2)/((1-r^2)^2+(2\zeta r)^2)]^{1/2} \quad (1)$$

where: y_1 (m) is the displacement amplitude on the input side of the tested sample, y_2 (m) is the displacement amplitude on the output side of the tested sample, ζ (–) is the damping ratio and r (–) is the frequency ratio. The damping and frequency ratios are given by the formulas (2) and (3) (Rao, 2005; Stephen, 2005; Yu et al., 2018):

$$\zeta=c/(4km)^{1/2} \quad (2)$$

$$r=\omega/\omega_n=\omega/(k/m)^{1/2} \quad (3)$$

where: c (N·s/m) is the viscous damping coefficient, k (N/m) is the spring constant, m (kg) is the mass, ω (rad/s) is the frequency of oscillation and ω_n (rad/s) is the undamped natural frequency.

Under the condition $dT_d/dr=0$ in the equation (1), it is possible to determine the frequency ratio r_0 at which the displacement transmissibility T_d has its maximum value:

$$r_0=[(1+8\zeta^2)^{1/2}-1]^{1/2}/(2\zeta) \quad (4)$$

It is evident from the equation (4) that the local extrema of the displacement transmissibility is generally shifted to lower values of the frequency ratio r with the increasing damping ratio ζ (or with the decreasing spring constant k). In this study, the vibration damping properties of the investigated rubber composites were evaluated by means of the transfer damping function D (dB) which is expressed in the case of harmonically excited vibration as follows, equation (5):

$$D=20\cdot\log(a_1/a_2)=20\cdot\log(1/T_d) \quad (5)$$

where: a_1 (m/s^2) is the acceleration amplitude on the input side of the tested sample and a_2 (m/s^2) is the acceleration amplitude on the output side of the tested sample. Based on the transfer damping function value, there are three different types of mechanical vibration, i.e. resonance (D<0), undamped (D=0) and damped (D>0) vibration.

The acceleration amplitudes a_1 and a_2 were recorded by BK 4393 accelerometers A_1 and A_2 (see Figure 1). Measurements of the transfer damping function were performed for different inertial masses m (i.e. for 0, 85 and 500 g), which were placed on the upper side of the harmonically loaded sample (see Figure 1). Moreover, vibration damping properties of the investigated rubber samples with the ground plane dimensions 60×60 mm were performed for two different material thicknesses (i.e. for 10 mm and 20 mm). Each measurement was repeated 5 times at the ambient temperature of 23 °C.

4. RESULTS AND DISCUSSION

Basic mechanical properties (namely the modulus of elasticity E_{50} at 50% sample extension, the Shore A hardness and the rebound resilience R) of the investigated rubber composite materials are shown in Table 3. It is evident that higher concentrations of the applied nanofillers lead generally to an increased rubber stiffness, which is manifested by higher values of the modulus of elasticity E_{50} and the Shore A hardness. Contrariwise, the rubber rebound resilience R decreases with the increasing concentration of the used nanofillers.

Table 3. Mechanical properties of the investigated rubber samples

Rubber sample	E_{50} [MPa]	Shore A [Sh A]	R [%]
0_0	0.60±0.06	38±1	56±1
50_0	1.32±0.06	55±1	39±1
40_10	1.33±0.05	57±1	32±1
30_20	1.40±0.06	59±1	24±1
20_30	1.54±0.14	62±1	17±1

The tested rubber composites were subsequently investigated in terms of their viscoelastic behaviour. The storage modulus E´, the loss modulus E´´ and the loss factor tanδ were investigated depending on the excitation frequency f and the sample deformation x under cyclic tensile load.

Frequency dependencies of the storage modulus E´ and the loss modulus E´´ of the investigated rubber samples at the sample deformation x=10µm and the temperature t=25°C are shown in Figure 2 and Figure 3. It is visible that the lowest values of the storage and loss moduli independently of the excitation frequency were obtained for the rubber sample 0_0 that was produced without the applied nanofillers. Furthermore, the storage and loss moduli are increasing with the increasing concentration of the used nanofillers, mainly with the increasing concentration of the Cloisite 20A nanofiller.

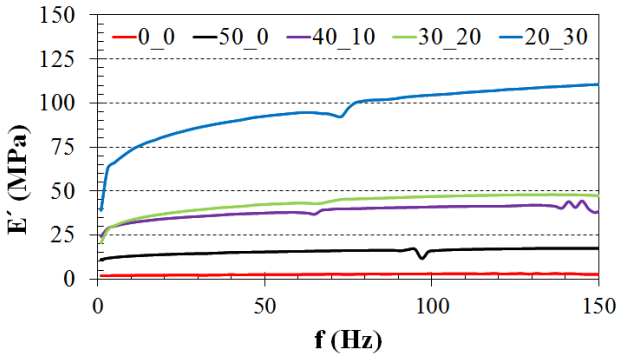

Fig. 2. Frequency dependencies of the storage modulus of the tested rubber samples at the sample deformation x=10 µm and the temperature t=25°C

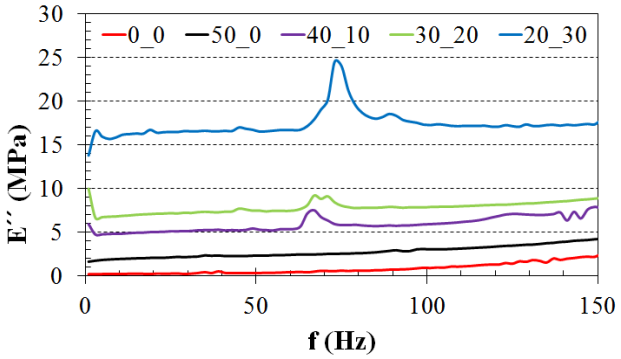

Fig. 3. Frequency dependencies of the loss modulus of the tested rubber samples at the sample deformation x=10 µm and the temperature t=25°C

The stiffness and damping properties of materials are also dependent on the operating temperature. The effect of the operating temperature on frequency dependencies of the storage and loss moduli for two different rubber samples is demonstrated in Figure 4. It is obvious that higher values of the storage and loss moduli are obtained at the lower operating temperature (at t=25°C). Similar frequency dependencies were found for all other investigated types of the rubber composites. It is because the higher operating temperature leads to a decrease of the stiffness and to a decrease of energy dissipation under harmonic loading of the tested rubber materials.

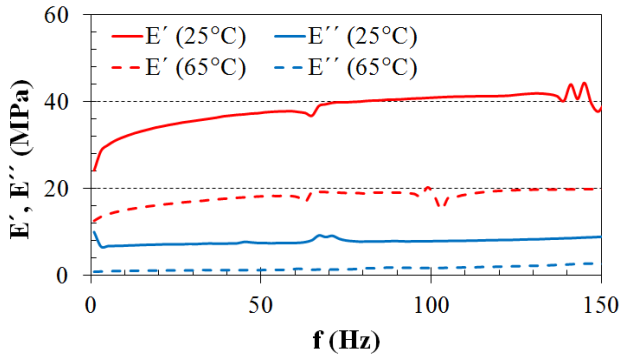

Fig. 4. Effect of the operating temperature on frequency dependencies of the storage and loss moduli at the sample deformation x=10 µm (red lines – sample 40_10, blue lines – sample 30_20)

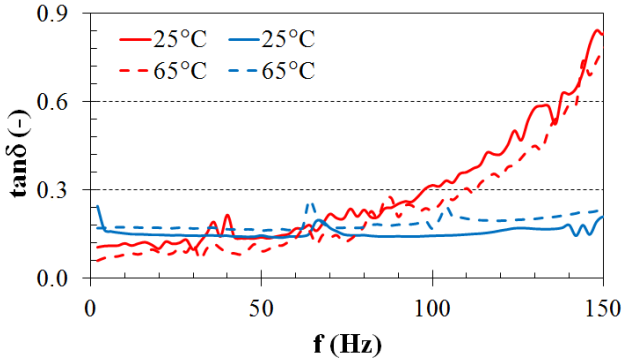

Fig. 5. Effect of the operating temperature on frequency dependencies of the loss factor at the sample deformation x=10 µm (red lines – sample 0_0, blue lines – sample 40_10)

As mentioned above, damping properties of materials under dynamic loading are characterized by the loss factor tanδ. Examples of frequency dependencies of the loss factor for two rubber samples at two different operating temperatures are presented in Figure 5. It is evident that their composition, the excitation frequency and the operating temperature significantly influence damping properties of the investigated rubber composites. It was found in this study that higher values of the loss factor were observed for the sample 0_0, namely at higher excitation frequencies (f>75 Hz). Damping properties decreased gradually

with the increasing concentration of the applied nanofillers in the frequency range from 75Hz to 150Hz (Figure 5). On the contrary, the rubber samples with higher concentrations of the nanofillers embodied generally higher energy dissipation at lower excitation frequencies (f<75 Hz). It was also found, that rubber samples with higher concentrations of the nanofillers achieve better damping properties at the higher operating temperature (t=65°C). Contrariwise, the rubber sample produced without nanofillers (sample 0_0) and the rubber sample filled only with the carbon black N 320 nanofiller (sample 50_0) are more suitable at the lower operating temperature (t=25°C) in terms of higher energy dissipation into heat under dynamic loading.

Furthermore, deformation dependencies of the viscoelastic parameters were also investigated depending on the excitation frequency and the operating temperature under harmonic loading of the tested rubber composites. Deformation dependencies of the storage and loss moduli at the excitation frequency of 1Hz and the operating temperature of 65°C for selected rubber composites are shown in Figure 6. It is apparent that higher values of these moduli are again obtained at higher concentrations of the applied nanofillers that contribute to an increase of the rubber stiffness and energy dissipation into heat. It is also evident from Figure 6 that the maximum value of the loss modulus (the point A) is obtained at a given sample deformation depending on the rubber type. It is caused by the highest interactive forces between macromolecules of the given rubber and the nanofillers (Wu et al., 2005).

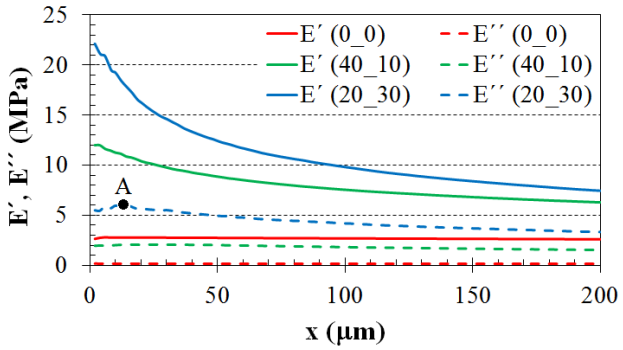

Fig. 6. Deformation dependencies of the storage and loss moduli at the excitation frequency f=1Hz and the temperature t=65°C

The effect of the excitation frequency and the operating temperature on deformation dependencies of the storage and loss moduli for the rubber sample 50_0 is shown in Figure 7. It is visible that higher values of these moduli are generally obtained at the higher excitation frequency (f=20Hz) and the lower operating temperature (t=25°C). Similar results were found for all other types of the tested rubber samples.

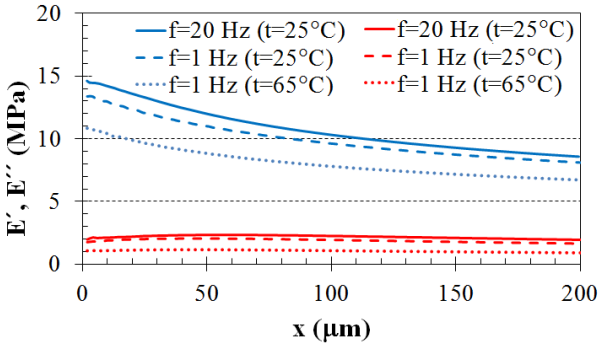

Fig. 7. Effect of the excitation frequency and the operation temperature on deformation dependencies of the storage and loss moduli for the sample 50_0 (blue lines – storage modulus, red lines – loss modulus)

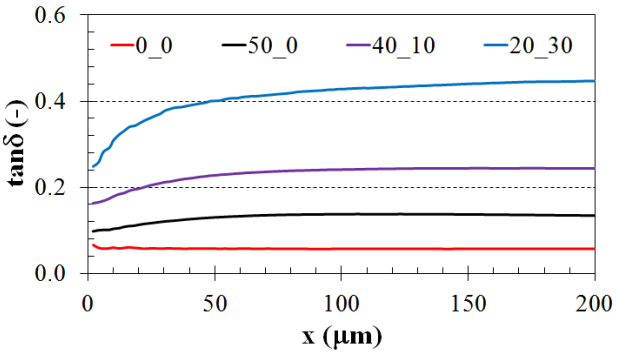

Fig. 8. Deformation dependencies of the loss factor at the excitation frequency f=1 Hz and the temperature t=65°C

Deformation dependencies of the loss factor at the excitation frequency f=1Hz and the operating temperature t=65°C are shown in Figure 8. It is evident from this comparison that a higher ability to dissipate input mechanical energy into heat was generally obtained in the case of the rubber mixtures that were filled with the applied nanofillers. It is given by the fact that more nanofiller particles in the rubber mixtures result in a higher internal friction between the particles and subsequently in higher energy dissipation under dynamic loading of these mixtures. A lamellar shape of the Cloisite 20A nanofiller mainly causes it.

The effect of the operating temperature and the excitation frequency on deformation dependencies of the loss factor was similar to the measured deformation dependencies of the storage and loss moduli (Figure 7). It was found (Figure 9) that a higher internal friction under harmonic loading of the tested rubber mixtures was again obtained at the higher excitation frequency (f=20Hz) and the lower operating temperature (t=25°C).

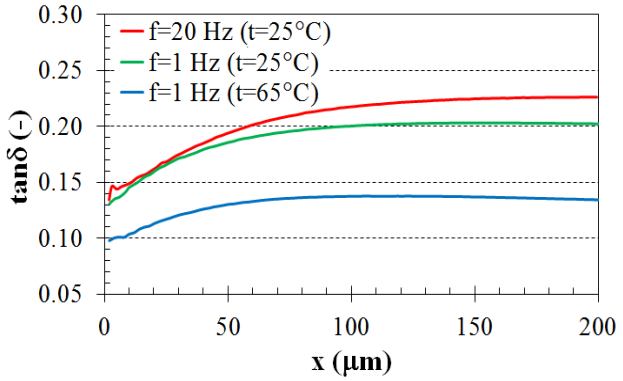

Fig. 9. Effect of the excitation frequency and the operation temperature on deformation dependencies of the loss factor for the sample 50_0

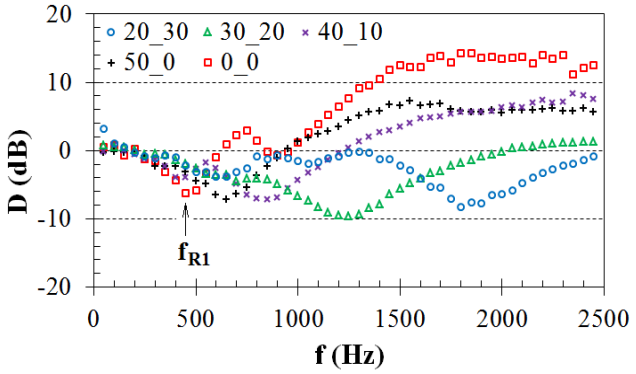

Fig. 10. Frequency dependencies of the transfer damping function of the investigated rubber samples (thickness t=10 mm, inertial mass m=85g)

Finally, the rubber composite materials were investigated in terms of their ability to damp mechanical vibration. The effect of the rubber composition on vibration damping properties of the tested rubber samples is shown in Figure 10. It is evident from this comparison that the rubber composition has a significant influence on vibration damping properties. It can be concluded that the best vibration damping (i.e. for D>0) was obtained for the sample without the applied nanofillers (sample 0_0). On the contrary, the material ability to damp mechanical vibration decreases with the increasing concentrations of the used nanofillers. It is caused by the increasing stiffness of the filled rubber composites. It is visible (see Figure 10) that the first resonance frequency ($f_{R1} \approx D_{min}$) peak position is shifted to higher excitation frequencies with increasing the rubber stiffness. This fact is consistent with the equation (4). The values of the first resonance frequency f_{R1} of the studied composite materials for different rubber thicknesses and inertial masses are shown in Table 4.

Table 4. First resonance frequency f_{R1} in Hz of the studied rubber composites under harmonic excitation for different rubber thicknesses t and inertial masses m

Rubber sample	t [mm]	m (g)		
		0	85	500
0_0	10	885±22	472±15	256±11
	20	236±9	231±8	176±6
50_0	10	1293±26	650±16	292±13
	20	487±15	425±14	230±8
40_10	10	1712±34	844±18	301±14
	20	536±13	474±12	250±10
30_20	10	2056±41	1265±27	310±11
	20	563±14	508±11	304±9
20_30	10	2549±46	1870±35	321±12
	20	700±17	645±15	305±11

Vibration damping properties are also influenced by the inertial mass, which is placed on the upper side of the tested samples (Figure 1). The influence of the inertial mass on the transfer damping function for the sample 40_10 of the thickness t=10mm is shown in Figure 11. It is evident that better damping properties were generally obtained for higher inertial masses m, which is reflected by a decrease of the undamped natural frequency ω_n (see the equation (3)) and by a shift of the first resonance frequency peak position to lower excitation frequencies (Table 4).

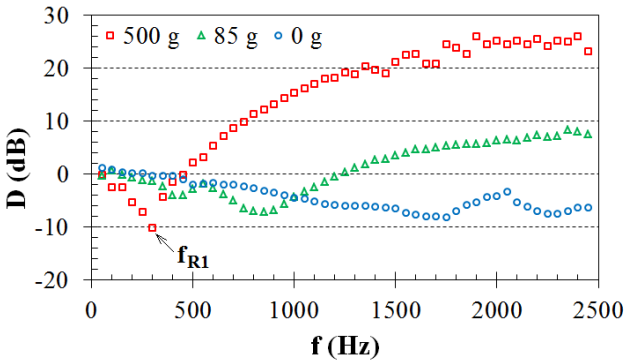

Fig. 11. Frequency dependencies of the transfer damping function for the sample 40_10 of the thickness t=10 mm loaded with different inertial masses.

The influence of the rubber thickness on vibration damping of the sample 30_20, which was loaded with the inertial mass m=85g, is shown in Figure 12. It is visible that the higher rubber thickness leads to a shift of the first resonance frequency peak position to the left (Table 4). Therefore, the rubber thickness has a positive influence on vibration damping. It is caused by a higher internal friction of thicker materials (t=20mm) under dynamic loading compared to the rubber composites of the thickness t=10mm.

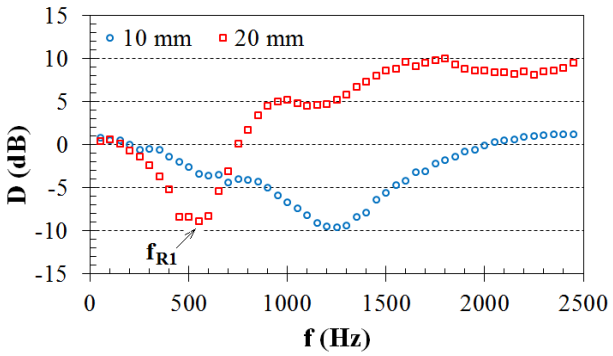

Fig. 12. Effect of the rubber thickness on frequency dependencies of the transfer damping function for the sample 30_20 loaded with the inertial mass m=85g.

It is visible from Figures 10-12 that the material ability to damp mechanical vibration is also significantly influenced by the excitation frequency. It is also obvious, that the resonance mechanical vibration (D<0) was generally observed at low excitation frequencies depending on the rubber type, its thickness and the inertial mass. For example for the sample 20_30 of the thickness t=10mm and without the inertial mass (m=0g), the resonant mechanical vibration was observed at the excitation frequencies f<2850Hz. In the case of the sample 0_0 of the thickness t=20mm and loaded with the inertial mass m=500g, the resonant mechanical vibration was achieved at considerably lower excitation frequencies (at f<440Hz). Contrariwise, the damped mechanical vibration (D>0) was generally achieved at higher excitation frequencies.

5. CONCLUSIONS

The aim of the paper was to study the mechanical properties of rubber composites that were filled with two types of nanofillers, namely with Cloisite 20A and carbon black N 320 nanofillers. It can be concluded that the mechanical properties of the investigated rubber samples are significantly influenced by their composition. Therefore, a specific type of rubber is suitable for certain application in practice.

The mechanical properties of the rubber mixtures were investigated on the basis of tensile, hardness, rebound resilience, viscoelastic and vibro-insulating properties. It was found in this work that the rubber stiffness generally increases with the increasing concentrations of the applied nanofillers, resulting in lower rebound resilience and higher hardness, storage and loss moduli of elasticity. It can be also stated that the storage and loss moduli decreased with the increasing operating temperature. The above-mentioned facts were in good agreement with the vibro-insulating measurements of the observed rubber materials that were examined by the method of forced oscillation based on the transfer damping function. The ability of materials to damp mechanical vibration under harmonic excitation is associated with the first resonance frequency, which is generally lower for materials with better vibration damping properties. It was found that the first resonance frequency peak position is shifted to higher excitation frequencies with increasing stiffness of the tested rubber mixtures, i.e. with increasing concentrations of the used nanofillers. For this reason, the rubber mixtures containing the nanofillers exhibit a lower ability to damp mechanical vibration compared to the non-filled rubber-like material. Therefore, the application of the used nanofillers in the rubber composites results in a lower transformation of input mechanical energy into heat under harmonically excited vibration of these rubber materials. It was further found in this study that the ability of materials to damp mechanical vibration generally increases with increasing excitation frequency, inertial mass and thickness of the investigated rubber mixtures.

In future work, it is possible to develop other types of rubber mixtures filled with different types of nanofillers and surface modified fillers in order to obtain required properties and suitable applications of these materials.

6. ACKNOWLEDGEMENTS

This work was supported by Research Centre of Advanced Mechatronic Systems project, project number CZ.02.1.01/0.0/0.0/16_019/0000867 within the Operational Programme Research, Development and Education, by the Scientific Grant Agency of the Ministry of Education of Slovak Republic and the Slovak Academy of Sciences under Project VEGA 1/0374/19 and by a grant IGA/FT/2018/008.

7. REFERENCES

1. Chandrasekaran, V. C., (2010). *Rubber properties for functional seal requirements*, Rubber seals for fluid and hydraulic systems, pp. 7-22, Elsevier, Oxford.

2. Cox, R. L., (2012). *Inorganic filler materials*, Engineered tribological composites – the art of friction material development, pp. 399-421, SAE International, London.

3. Eckhoff, R. K., (2016). *Gas and dust explosions caused by smoldering combustion in powder layers and deposits*, Explosion hazards in the process industries, pp. 233-252, Elsevier, Oxford.

4. Gent, A. N., (2012). *Materials and compounds*, Engineering with rubber – how to design rubber components, pp. 11-34, Hanser Publications, Cincinnati.

5. Ghari, H. S., Jalali-Arani, A., (2016).

Nanocomposites based on natural rubber, organoclay and nano-calcium carbonate: Study on the structure, cure behavior, static and dynamic-mechanical properties, Applied Clay Science, **119**(2), 348-357.
6. Lee, H. H., Abhijeet, S., Ilisch, S. et al., (2014). *The role of linked phospholipids in the rubber-filler interaction in carbon nanotube (CNT) filled natural rubber (NR),* Polymer, **55**(18), 4738-4747.
7. Limper, A., (2012). *Processing aspects of rubber mixing,* Mixing of rubber compounds, pp. 47-70, Hanser Publishers, Munich.
8. Mallik, A. K., Kher, V., Puri, M., Hatwal, H., (1999). *On the modelling of non-linear elastomeric vibration isolators,* Journal of Sound and Vibration, **219**(2), 239-253.
9. Rao, S. S., (2005). *Response of a damped system under the harmonic motion of the base,* Mechanical vibrations, pp. 281-287, Pearson, Upper Saddle River.
10. Reyes-Melo, E., Martinez-Vega, J., Guerrero-Salazar, C., Ortizs-Méndez, U., (2004). *On the modeling of the dynamic-elastic modulus for polymer materials under isochronal conditions,* Journal of Applied Polymer Science, **94**(2), 657-670.
11. Stephen, N. G., (2005). *On energy harvesting from ambient vibration,* Journal of Sound and Vibration, **293**(1-2), 409-425.
12. Thomas, S., Chan, C. H., Pothen, L. A., Joy, J. P., Maria, H. J., (2014). *Nanofillers in natural rubber*, Natural rubber materials, Volume 2 – Composites and nanocomposites, pp. 34-72, The Royal Society of Chemistry, Cambridge.
13. Valaderes, L. F., Leite, C. A. P., Galembeck, F., (2006). *Preparation of natural rubber-montmorillonite nanocomposite in aqueous medium: evidence for polymer-platelet adhesion,* Journal of Polymer, **47**(2), 672-678.
14. Wu, Y. P., Wang, Y. Q., Zhang, H. F., Wang, Y. Z., Yu, D. S., Zhang, L. Q., Yang, J., (2005). *Rubber-pristine clay nanocomposites prepared by co-coagulating rubber latex and clay aqueous suspension,* Composites Science and Technology, **65**(7-8), 1195-1202.
15. Wu, Y. T., Mark, J. E., Pham, L. H., Engelhardt, M., (2001). *Clay nanolayer reinforcement of cis-1,4-polyisoprene and epoxidized natural rubber,* Journal of Applied Polymer Science, **82**(6), 1391-1403.
16. Yu, H. J., Xu, Y. H., Sun, X. T., (2018). *Analysis of the non-linear vibration isolation system with dry friction,* Journal of Mechanical Science and Technology, **32**(4), 1489-1497.

Received: April 10, 2019 / Accepted: December 20, 2019 / Paper available online: December 25, 2019